

Privacy-Protecting Energy Management Unit through Model-Distribution Predictive Control

Jun-Xing Chin, *Student Member, IEEE*, Tomas Tinoco De Rubira, and Gabriela Hug, *Senior Member, IEEE*

Abstract—The roll-out of smart meters in electricity networks introduces risks for consumer privacy due to increased measurement frequency and granularity. Through various Non-Intrusive Load Monitoring techniques, consumer behavior may be inferred from their metering data. In this paper, we propose an energy management method that reduces energy cost and protects privacy through the minimization of information leakage. The method is based on a Model Predictive Controller that utilizes energy storage and local generation, and that predicts the effects of its actions on the statistics of the actual energy consumption of a consumer and that seen by the grid. Computationally, the method requires solving a Mixed-Integer Quadratic Program of manageable size whenever new meter readings are available. We simulate the controller on generated residential load profiles with different privacy costs in a two-tier time-of-use energy pricing environment. Results show that information leakage is effectively reduced at the expense of increased energy cost. The results also show that with the proposed controller the consumer load profile seen by the grid resembles a mixture between that obtained with Non-Intrusive Load Leveling and Lazy Stepping.

Index Terms—Consumer Privacy, Energy Management Unit, Model Predictive Control, Mutual Information, Optimization Methods, Smart Meter

I. INTRODUCTION

Globally, traditional electromechanical electricity meters are being replaced by Smart Meters (SMs) as part of efforts to modernize the grid in order to better manage electricity generation and distribution. In Europe, this is mandated by the European Commission under its Third Energy Package, requiring member states to roll-out SMs where cost-benefit analyses are positive [1]. However, with their ability to provide real-time information on consumer demand, SMs also raise concerns regarding consumer privacy [2], [3]. By measuring energy demand at much higher frequencies than traditional meters, detailed consumer load profiles can be extracted from SM data. Through Non-Intrusive Load Monitoring (NILM) techniques, which were first studied by Hart in 1989 [4] and further developed through the years [5], [6], individual appliance usage, and ultimately consumer lifestyle patterns, preferences, and occupancy profiles can be inferred [7]–[9]. Such data may not only be accessible to Utility Providers (UPs) but also to malicious third parties, as metering infrastructures are vulnerable to attacks that lead to information

leakage [10]. Moreover, if one also considers UPs being untrustworthy parties, privacy concerns stemming from SM roll-outs become much more severe, and can even lead to backlashes against their installation [11].

To counter this, various works have been done in order to protect consumer privacy. While some focus on cyber measures, such as encryption, adding noise to achieve differential privacy [12], and consumer aggregation, others address the problem through physical means, *e.g.*, load control [13] and battery load hiding (BLH) [14], [15]. BLH techniques mask consumer load by charging and discharging a battery to alter the load profile captured by SMs. For example, in [14], the authors use a best-effort algorithm to hide consumer load change, whilst [15] details a load-leveling method that switches its energy consumption based on the battery's state-of-charge. The authors in [16], on the other hand, introduce a stepping algorithm that improves upon the performance of best-effort and load-leveling algorithms. While privacy loss metrics, *e.g.*, Mutual Information and Fischer Information, have been used to assess BLH schemes such as in [16], the schemes themselves have been primarily heuristics-driven. Cyber-physical methods proposed for minimizing directly a specific privacy loss measure such as mutual information have so far been mainly theoretical [17], [18].

In general, BLH methods proposed in the literature for privacy protection have not directly considered energy cost in the control policies. Any cost savings obtained have been a by-product of the privacy protection scheme. In these methods, the level of privacy protection is closely linked to storage capacity [16], [19], but privacy protection alone is unlikely to justify the cost of investment on high-capacity storage devices, which according to estimates by [20] remains high. Utilizing energy storage for minimizing energy cost in addition to providing privacy protection is critical for justifying this investment. Methods that focus on minimizing energy cost alone have been the subject of many works. Examples of recent work include [21], [22], where the authors utilize batteries in a Model Predictive Control (MPC) scheme to minimize energy costs in a varying-price environment by charging during low-price periods to compensate consumer load during high-price periods.

In this paper, we propose a new scheme based on MPC that combines energy cost minimization with privacy protection that directly minimizes mutual information. The proposed scheme introduces binary variables in the MPC optimization subproblems for counting predicted observations and estimating the joint statistics of consumer load and the net load seen by the grid (grid load). This allows the controller to predict

This work was supported in part by the *Swiss National Science Foundation* for the COPEs project under the CHIST-ERA Resilient Trustworthy Cyber-Physical Systems (RTCPS) initiative, and in part by the *ETH Zurich Postdoctoral Fellowship FEL-11 15-1*.

J.X. Chin, T. Tinoco De Rubira, and G. Hug are with the Power Systems Laboratory, ETH Zurich, 8092 Zurich, Switzerland. Email: {chin | tomas | hug}@eeh.ee.ethz.ch.

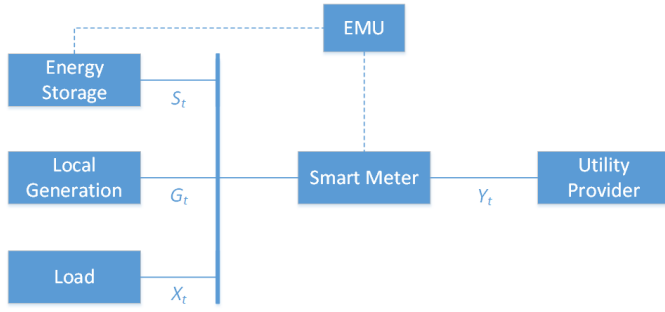


Fig. 1: Energy System Model.

the effects of its actions on the mutual information between these two load profiles. Computationally, the proposed scheme requires solving Mixed-Integer Quadratic Programs (MIQPs) of manageable size whenever new meter readings are available.

The rest of this paper is structured as follows: Section II describes the problem considered. Section III presents our proposed solution approach. Section IV details implementation and numerical experiments. Lastly, Section V summarizes this work and provides an outlook on future research.

II. PROBLEM DESCRIPTION

We consider the problem of minimizing energy cost and reducing information leakage about the load profile of an energy consumer. The system considered consists of an Energy Management Unit (EMU) that uses energy storage, local generation, and energy available from the grid to supply the consumer load in a cost-effective and privacy-concerned manner. This is illustrated in Fig. 1. Mathematically, the system is represented by the discrete-time random process

$$\{(S_t, G_t, C_t, X_t, Y_t) \mid t \in \mathbb{Z}_+\},$$

where S_t is the energy supplied to the energy storage, G_t is the energy supplied by the local generation, C_t is the price of energy, X_t is the consumer energy demand, and Y_t is the energy demand seen by the grid during time interval t , *i.e.*,

$$Y_t = X_t + S_t - G_t. \quad (1)$$

This implies that no energy wastage is allowed. The realizations of these random variables are denoted by s_t , g_t , c_t , x_t , and y_t , respectively, for each time t .

The battery charging energy S_t is constrained by

$$S^{\min} \leq S_t \leq S^{\max} \quad (2)$$

during each time interval t , where $-S^{\min} \geq 0$ is the maximum discharging energy and $S^{\max} \geq 0$ is the maximum charging energy at a constant power over a single time interval. These constraints are given by the power rating of the device. It is assumed that the charge and discharge efficiencies are equal, and we denote these with $\alpha \in (0, 1)$. The state of charge of the energy storage device at the beginning of time interval t is denoted by E_t and satisfies

$$E_{t+1} = E_t + \alpha \mathbb{1}\{S_t \geq 0\}S_t + \alpha^{-1} \mathbb{1}\{S_t < 0\}S_t, \quad (3)$$

for each t , where $\mathbb{1}\{A\} = 1$ when A is true and 0 otherwise. It is also assumed for simplicity that the energy storage device

is not used to provide ancillary services to the grid, allowing the full use of its capacity, and as such is constrained by

$$0 \leq E_t \leq E^{\max}, \quad (4)$$

where E^{\max} is the maximum energy storage capacity of the device. Additionally, it is assumed in our system that the local generation is deterministic in nature and that the EMU has perfect prior knowledge regarding its output. The future consumer loads X_t as well as the energy prices C_t are also assumed to be known to the EMU. In practice, only noisy predictions would be available but the incorporation of such uncertainties is part of a future work. With regards to the grid, we assume that no energy feed-in to the grid is allowed and that the energy supplied is bounded by Y^{\max} , the maximum connection capacity available on the distribution feeder cables (or circuit breakers), *i.e.*,

$$0 \leq Y_t \leq Y^{\max}. \quad (5)$$

The energy cost at each time interval t is given by $C_t Y_t$. On the other hand, loss of consumer privacy is measured by the information leakage rate of consumer load given grid load, which following [23] is given by

$$I(X^{[t]}; Y^{[t]}) := \int_X \int_Y p_{X,Y}(x_0, y_0, \dots, x_t, y_t) \times \log \frac{p_{X,Y}(x_0, y_0, \dots, x_t, y_t)}{p_X(x_0, \dots, x_t) p_Y(y_0, \dots, y_t)} dy dx.$$

Here, $X^{[t]} := (X_0, \dots, X_t)$, $Y^{[t]} := (Y_0, \dots, Y_t)$, $p_{X,Y}$, p_X and p_Y denote the probability density functions of $(X^{[t]}, Y^{[t]})$, $X^{[t]}$ and $Y^{[t]}$, respectively, and \log denotes the base-2 logarithm. Quantifying the cost of privacy loss through a non-negative constant μ with units of Rp-per-bit (100 Rp = 1 CHF), we seek to find a causal and implementable control policy $U \in \mathcal{U}$ that minimizes the total time-average expected cost. Such a policy determines the charge and discharge of the energy storage device during each time interval t based on the observation history up to that time, *i.e.*,

$$S_t = U(X^{[t]}, C^{[t]}, G^{[t]}, Y^{[t-1]}, S^{[t-1]}),$$

where $C^{[t]}$, $G^{[t]}$ and $S^{[t]}$ are defined in analogous ways to $X^{[t]}$ and $Y^{[t]}$. Mathematically, the problem can be posed as finding a policy U^* such that

$$U^* = \arg \min_{U \in \mathcal{U}} f(U), \quad (6)$$

where

$$f(U) := \lim_{\bar{T} \rightarrow \infty} \frac{1}{\bar{T} + 1} \left\{ \sum_{\tau=0}^{\bar{T}} \mathbb{E}[C_\tau Y_\tau] + \mu I(X^{[\bar{T}]}; Y^{[\bar{T}]}) \right\}$$

and $\mathbb{E}[\cdot]$ denotes expectation.

III. MODEL-DISTRIBUTION PREDICTIVE CONTROL

We propose an approach based on MPC to find a control policy that is close to U^* . At time t , the controller (EMU) observes the realizations x_t , g_t , c_t , and e_t (energy storage state of charge), determines actions s_t, \dots, s_{t+T} for a prediction horizon of length T , executes action s_t to achieve a desirable

grid load y_t , and repeats the process in a receding horizon manner.

Since the exact evaluation of the information leakage rate $I(X^{[t]}; Y^{[t]})$ is not possible without knowing the probability density functions $p_{X,Y}$ and p_Y , which depend on the control actions, we propose using an approximation. This is done by first assuming that for τ near time t , (X_τ, Y_τ) are independent identically distributed (i.i.d.) samples of a pair of random variables $(\tilde{X}_t, \tilde{Y}_t)$. More specifically, this is assumed during the time window $\{t + T - N + 1, \dots, t + T\}$, which has length $N \gg T$ and covers both the recent past and the entire prediction horizon with respect to time t . While time independence does not hold in reality, we make this strong assumption as a first step in making the problem tractable. Time correlation and other properties will be studied in future work. Letting $X^{[t]} := (X_{t-M+1}, \dots, X_{t+T})$ and $Y^{[t]} := (Y_{t-M+1}, \dots, Y_{t+T})$, where $M := N - T$, and approximating the average information leakage per time interval using

$$\frac{I(X^{[t+T]}; Y^{[t+T]})}{t + T + 1} \approx \frac{I(X^{[t]}; Y^{[t]})}{N},$$

the locally i.i.d. assumption then gives that

$$\begin{aligned} \frac{I(X^{[t+T]}; Y^{[t+T]})}{t + T + 1} &\approx \frac{I(X^{[t]}; Y^{[t]})}{N} \\ &= \sum_{\tau=t-M+1}^{t+T} \frac{I(X_\tau; Y_\tau)}{N} \\ &= \sum_{\tau=t-M+1}^{t+T} \frac{I(\tilde{X}_t; \tilde{Y}_t)}{N} \\ &= I(\tilde{X}_t, \tilde{Y}_t), \end{aligned} \quad (7)$$

where first equality stems from time independence, and the second equality from the random variables being identically distributed.

Furthermore, for the purpose of approximating mutual information only, we assume that the random variables \tilde{X}_t and \tilde{Y}_t can take on only a finite number of energy levels that are evenly spaced by 2Δ , i.e., $\tilde{X}_t \in \{x^1, x^2, \dots, x^m\}$ and $\tilde{Y}_t \in \{y^1, y^2, \dots, y^n\}$, where $x^1 - \Delta = 0$, $x^m + \Delta = X^{\max}$, $y^1 - \Delta = 0$, and $y^n + \Delta = Y^{\max}$. The value X^{\max} can be computed from historical records. From this assumption, it follows that

$$\begin{aligned} I(\tilde{X}_t; \tilde{Y}_t) &= \sum_{i=1}^m \sum_{j=1}^n p_{\tilde{X}, \tilde{Y}}(x^i, y^j) \log \frac{p_{\tilde{X}, \tilde{Y}}(x^i, y^j)}{p_{\tilde{X}}(x^i) p_{\tilde{Y}}(y^j)} \\ &= \sum_{i=1}^m \sum_{j=1}^n p_{\tilde{X}, \tilde{Y}}(x^i, y^j) \log \frac{p_{\tilde{Y}|\tilde{X}}(y^j|x^i)}{p_{\tilde{Y}}(y^j)}, \end{aligned} \quad (8)$$

where $p_{\tilde{X}, \tilde{Y}}$, $p_{\tilde{X}}$, $p_{\tilde{Y}}$ and $p_{\tilde{Y}|\tilde{X}}$ denote the probability mass functions of $(\tilde{X}_t, \tilde{Y}_t)$, \tilde{X}_t , \tilde{Y}_t and \tilde{Y}_t given \tilde{X}_t , respectively. Since (X_τ, Y_τ) are assumed to be i.i.d samples of $(\tilde{X}_t, \tilde{Y}_t)$ for $\tau \in \{t + T - N + 1, \dots, t + T\}$, the statistics of these random variables are approximated by the relative frequency

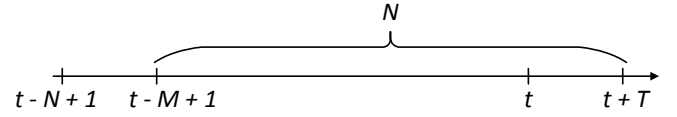


Fig. 2: Counting window for probability estimation at time t .

of events during this time window, as illustrated in Fig. 2. More specifically,

$$\begin{aligned} p_{\tilde{X}, \tilde{Y}}(x^i, y^j) &\approx \frac{\sum_{\tau=t-M+1}^{t+T} \mathbf{1}\{(x_\tau, y_\tau) = (x^i, y^j)\} + \varepsilon}{N + mn\varepsilon} \\ p_{\tilde{X}}(x^i) &\approx \frac{\sum_{\tau=t-M+1}^{t+T} \mathbf{1}\{x_\tau = x^i\} + n\varepsilon}{N + mn\varepsilon} \\ p_{\tilde{Y}}(y^j) &\approx \frac{\sum_{\tau=t-M+1}^{t+T} \mathbf{1}\{y_\tau = y^j\} + m\varepsilon}{N + mn\varepsilon}, \end{aligned}$$

where $\varepsilon > 0$. The addition of the positive scalar ε in the probability estimates corresponds to additive smoothing [24]. This is done to avoid probability estimates of zero for events for which there are no observations during the time window. This probability estimation strategy, albeit simplistic, constitutes an adequate choice for a first step towards exploring the proposed methodology of including in MPC the ability to estimate the statistical effects of the control actions in a tractable manner. Including more sophisticated probability estimation techniques into this methodology is an interesting subject for future work.

Since at time t the counting window covers the recent past and the prediction horizon, the probability estimates can be separated into parts that are constants and parts that depend on the controller's actions during the prediction horizon. More specifically, they can be expressed as

$$p_{\tilde{X}, \tilde{Y}}(x^i, y^j) \approx a_t^{ij} + \frac{1}{N_\varepsilon} \sum_{\tau=t}^{t+T} z_\tau^{ij} \quad (9)$$

$$p_{\tilde{Y}}(y^j) \approx b_t^j + \frac{1}{N_\varepsilon} \sum_{\tau=t}^{t+T} \sum_{k=1}^m z_\tau^{kj}, \quad (10)$$

where $N_\varepsilon := N + mn\varepsilon$, a_t^{ij} and b_t^j are constants (at time t) defined by

$$a_t^{ij} := \frac{\sum_{\tau=t-M+1}^{t-1} \mathbf{1}\{(x_\tau, y_\tau) = (x^i, y^j)\} + \varepsilon}{N_\varepsilon}$$

$$b_t^j := \frac{\sum_{\tau=t-M+1}^{t-1} \mathbf{1}\{y_\tau = y^j\} + m\varepsilon}{N_\varepsilon},$$

and $z_\tau^{ij} := \mathbf{1}\{(x_\tau, y_\tau) = (x^i, y^j)\}$ for $\tau \in \{t, \dots, t + T\}$, $i \in \{1, \dots, m\}$ and $j \in \{1, \dots, n\}$ are binary variables that depend on the controller's actions and forecasts during the prediction horizon. Letting $c_t^i := p_{\tilde{X}}(x^i)$, which is a constant at time t due to the perfect prediction assumption on consumer load, it follows from (9) and (10) that

$$p_{\tilde{Y}|\tilde{X}}(y^j|x^i) \approx \frac{a_t^{ij}}{c_t^i} + \frac{1}{c_t^i N_\varepsilon} \sum_{\tau=t}^{t+T} z_\tau^{ij}.$$

From these expressions for probability estimates and (8), we then have the approximation

$$\begin{aligned} I(\tilde{X}_t; \tilde{Y}_t) &\approx \bar{I}(\tilde{X}_t; \tilde{Y}_t) \\ &:= \sum_{i=1}^m \sum_{j=1}^n \left(a_t^{ij} + \frac{1}{N_\varepsilon} \sum_{\tau=t}^{t+T} z_\tau^{ij} \right) \times \\ &\quad \left\{ \log \left(a_t^{ij} + \frac{1}{N_\varepsilon} \sum_{\tau=t}^{t+T} z_\tau^{ij} \right) - \right. \\ &\quad \left. \log \left(b_t^j + \frac{1}{N_\varepsilon} \sum_{\tau=t}^{t+T} \sum_{k=1}^m z_\tau^{kj} \right) - \log c_t^i \right\}, \quad (11) \end{aligned}$$

which is a fairly complicated function of the binary variables z_τ^{ij} . Since $N \gg T$, this approximation can be simplified by replacing the logarithms with their first-order Taylor expansions around the constant part of their arguments, *i.e.*,

$$\begin{aligned} \log \left(a_t^{ij} + \frac{1}{N_\varepsilon} \sum_{\tau=t}^{t+T} z_\tau^{ij} \right) &\approx \log a_t^{ij} + \\ &\quad \log' (a_t^{ij}) \left(\frac{1}{N_\varepsilon} \sum_{\tau=t}^{t+T} z_\tau^{ij} \right) \\ \log \left(b_t^j + \frac{1}{N_\varepsilon} \sum_{\tau=t}^{t+T} \sum_{k=1}^m z_\tau^{kj} \right) &\approx \log b_t^j + \\ &\quad \log' (b_t^j) \left(\frac{1}{N_\varepsilon} \sum_{\tau=t}^{t+T} \sum_{k=1}^m z_\tau^{kj} \right). \end{aligned}$$

Using these Taylor expansions and letting $\nu := 1/\log_e 2$, we obtain the approximation

$$\begin{aligned} I(\tilde{X}_t; \tilde{Y}_t) &\approx \bar{I}(\tilde{X}_t; \tilde{Y}_t) \\ &:= \sum_{i=1}^m \sum_{j=1}^n \left(a_t^{ij} + \frac{1}{N_\varepsilon} \sum_{\tau=t}^{t+T} z_\tau^{ij} \right) \times \\ &\quad \left\{ \log \frac{a_t^{ij}}{b_t^j c_t^i} + \frac{\nu}{a_t^{ij} N_\varepsilon} \sum_{\tau=t}^{t+T} z_\tau^{ij} - \right. \\ &\quad \left. \frac{\nu}{b_t^j N_\varepsilon} \sum_{\tau=t}^{t+T} \sum_{k=1}^m z_\tau^{kj} \right\}, \quad (12) \end{aligned}$$

which is now a quadratic function of the binary variables z_τ^{ij} .

An important observation is that the curvature of the logarithm functions grows rapidly as zero is approached. Since the constants a_t^{ij} and b_t^j can be potentially very small for some i and j due to the absence of observations of the associated events in the time window $\{t-M+1, \dots, t-1\}$ and a poor choice of ε for additive smoothing, the Taylor expansions of the logarithms can be very poor. Hence, we propose choosing a bound ρ for $\log' (a_t^{ij})$ and $\log' (b_t^j)$ that ensures that the logarithms are always expanded sufficiently away from zero. Since

$$\log' (a_t^{ij}) = \frac{\nu}{a_t^{ij}} \leq \frac{N + mn\varepsilon}{\varepsilon} \nu$$

and

$$\log' (b_t^j) = \frac{\nu}{b_t^j} \leq \frac{\nu}{a_t^{ij}} = \log' (a_t^{ij}),$$

it follows that setting $\varepsilon \geq N/(\rho\nu^{-1} - mn)$ ensures that both $\log' (a_t^{ij})$ and $\log' (b_t^j)$ are always bounded by ρ .

Using (7) and the definition of $\bar{I}(\tilde{X}_t; \tilde{Y}_t)$, the ideal objective function for the MPC optimization problem that exactly captures energy cost minimization and privacy protection is approximated as follows:

$$\begin{aligned} &\frac{1}{T+1} \sum_{\tau=t}^{t+T} c_\tau y_\tau + \frac{1}{T+t+1} \mu I(X^{[t+T]}; Y^{[t+T]}) \\ &\approx \frac{1}{T+1} \sum_{\tau=t}^{t+T} c_\tau y_\tau + \mu \bar{I}(\tilde{X}_t; \tilde{Y}_t). \end{aligned}$$

Hence, the proposed MPC scheme consists of solving at each time t the optimization problem

$$\begin{aligned} &\underset{s, e, y, z, w}{\text{minimize}} \quad \frac{1}{T+1} \sum_{\tau=t}^{t+T} c_\tau y_\tau + \mu \Phi(z) \quad (13) \\ &\text{subject to} \quad (s, e, y, z, w) \in \mathcal{F}_t, \end{aligned}$$

where $\Phi(z) := \bar{I}(\tilde{X}_t; \tilde{Y}_t)$ measures privacy loss,

$$s := \{s_\tau\}_{\tau=t}^{t+T}, \quad e := \{e_\tau\}_{\tau=t}^{t+T}, \quad y := \{y_\tau\}_{\tau=t}^{t+T}$$

are continuous optimization variables, z is the collection of binary optimization variables defined by

$$\begin{aligned} z := &\left\{ z_\tau^{ij} \mid \tau \in \{t, \dots, t+T\}, \right. \\ &j \in \{1, \dots, n\}, \\ &\left. i = \arg \min_{k \in \{1, \dots, m\}} \|x_\tau - x^k\|_2 \right\}, \end{aligned}$$

and $w := \{w_\tau\}_{\tau=t}^{t+T}$ are binary variables used to represent the indicator functions in (3). Note that not all binary variables used in (11) are treated as optimization variables in (13). This is because many of them are known by the controller to be zero at time t since x_τ is assumed to be known, and for each $\tau \in \{t, \dots, t+T\}$, there is exactly one i such that

$$i = \arg \min_{k \in \{1, \dots, m\}} \|x_\tau - x^k\|_2.$$

The constraint $(s, e, y, z, w) \in \mathcal{F}_t$ enforces the binary restrictions on z and w , the system constraints (1)-(5), the constraint

$$\sum_{j=1}^n z_\tau^{ij} = 1 \quad (14)$$

for each $\tau \in \{t, \dots, t+T\}$, and the constraint

$$z_\tau^{ij} = 1 \iff j = \arg \min_{k \in \{1, \dots, n\}} \|y_\tau - y^k\|_2 \quad (15)$$

for each $\tau \in \{t, \dots, t+T\}$ and $j \in \{1, \dots, n\}$. Due to (14), the constraints (5) and (15) can be represented together by the linear constraints

$$\sum_{k=1}^n z_\tau^{ik} y^k - \Delta \leq y_\tau < \sum_{k=1}^n z_\tau^{ik} y^k + \Delta.$$

Problem (13) is therefore an MIQP with $(n+1)(T+1)$ binary variables, roughly $3(T+1)$ continuous variables, and roughly

$9(T + 1)$ linear constraints. Problem (13) is also recursively feasible [25] as long as the maximum consumer energy demand is less than the maximum allowable grid energy demand, *i.e.*, $X^{\max} \leq Y^{\max}$, and if generation curtailment is allowed. This stems from the fact that the grid can make up for any energy shortfall, local generation in excess of consumption and storage is curtailable, and mutual information is penalised in the objective function and not formulated as a constraint. In this work, generation curtailment is not considered as local generation is assumed to be deterministic and zero; but this can easily be included.

Since this proposed MPC scheme predicts the effects of the controller's actions on the probability distribution of random variables, we refer to it as Model-Distribution Predictive Control, or MDPC.

IV. NUMERICAL EXPERIMENTS

The proposed scheme was implemented in YALMIP [26] and MATLAB R2015a using the IBM CPLEX 12.6.3 solver. Simulations were done using consumer load profiles generated with tools from [27] over a period of approximately one month (30 days) with hourly resolution in a two-tier time-of-use energy pricing environment. The computer used for the simulations was an Intel Core i7-2600 CPU with 3.40 GHz of clock speed, and 16.0 GB of RAM.

In order to solve the MIQP problems (13) reliably and reduce the number of solution candidates, a convex penalty term $r(y)$ based on the l_1 -norm was added to the objective function. This is given by

$$r(y) = \frac{\mu\sigma T^{-1} \|Qy - \bar{y}\|_1}{\gamma(\|Qx - \bar{x}\|_1 + \|Qg - \bar{g}\|_1) + 1},$$

where σ and γ are positive constants, and y , x and g are grid load, consumer load and local generation vectors used in problem (13) for time t . The matrix Q extracts components that correspond to times $t, \dots, t+T-1$, and \bar{y} , \bar{x} , and \bar{g} denote values of Y_τ , X_τ , and G_τ for $\tau = t, \dots, t+T-1$ predicted during the solution of problem (13) for time $t-1$. This term is normalised for the prediction horizon length, and designed to encourage the controller to choose a set of actions at time t that is similar to those predicted at time $t-1$ in the absence of forecast errors. The values of σ and γ may be chosen such that $r(y)$ does not dominate the objective function, and hence are dependent on the characteristics of a particular data set. Note that the value of γ is negligible for this work as generation is assumed to be zero and the consumer load is perfectly known, *i.e.*, there are no forecast errors. Without the $r(y)$ term, the MIQP solver would spend an excessive amount of time performing branch-and-bound searches and utilize excessive memory resources trying to solve certain instances of (13).

Unless stated otherwise, the parameters shown in Table I were used for the simulations. Local generation was set to zero throughout the entire simulation period in order to clearly observe the effects of the controller actions. A battery was used as the energy storage device, and the parameters chosen were those of a Tesla Powerwall.

TABLE I: Default Simulation Parameters.

T :	12	Reg. Coefficient, σ :	0.11
M :	120	Battery Capacity:	6.4 kWh
N :	132	Battery Power:	3.3 kW
m :	15	Battery Efficiencies, α :	96 %
n :	15	Energy Price (high):	24.6 Rp/kWh
ε :	0.1	Energy Price (low):	13.15 Rp/kWh

A. Visualization of Load Profiles and Control Actions

Fig. 3 illustrates the actual consumer load and the load seen by the grid over seven days for two different prices of privacy loss, $\mu = 0$ and $\mu = 18$. For $\mu = 0$, the controller optimizes for energy costs only, and thus charges the battery during low-price periods and compensates consumer load during the high-price periods. This can be seen in Fig. 4(a) and 4(b), which show the charge and discharge of the battery, and the battery state of charge over a period of seven days. Periods highlighted in green indicate low-price periods. With the chosen horizon length of 12, the controller is unable to fully utilize the battery's capacity as the consumer load "seen" by it is generally less than the battery's capacity. With a price of privacy loss of $\mu = 18$, the controller now charges over high-price periods as well, as seen in Fig. 4(a), in order to mask low consumer load periods. This results in a grid load curve that shows a stepping behavior similar to that obtained in [16], with periods of load leveling similar to those obtained in [15]. Note that the correlation and thus also the mutual information of consumer and grid loads is greatly reduced for $\mu = 18$. This can be seen more clearly in Fig. 5, which illustrates the estimated distribution of $(\tilde{X}_t, \tilde{Y}_t)$. For $\mu = 18$ (right plot), the grid load concentrates in the two levels despite consumer load levels being spread out. For $\mu = 0$, while correlation between \tilde{X}_t and \tilde{Y}_t is reduced by the battery charging during low-price hours to compensate consumption during high-price hours, it is still possible for an adversary to reconstruct the consumer load based on observations of the grid load with knowledge of energy prices and the battery system specifications, as discussed in [16].

B. Performance of the MDPC Scheme

The proposed scheme was evaluated using $\bar{I}(\tilde{X}_t; \tilde{Y}_t)$, equivalently (11), with a static window of length $N = 718$ that encompasses the entire simulation period of approximately 30 days. This "cumulative" approximation of mutual information is denoted by I_c . For reference, a system without a battery using the same simulation setup had a total energy consumption of 534 kWh, energy costs of 125 CHF, and privacy loss of $I_c = 2.58$ bits.

In Fig. 6, the total energy costs and mutual information I_c for different battery capacities are shown as a function of the price μ of privacy loss. As can be seen from the figure, energy costs increase with the drop in mutual information, as the battery charges during high-price periods to mask low consumer loads, as previously shown in Fig. 4(a). While it would be possible for consumer behavior to be inferred with $\mu = 0$, the mutual information value with a 3.3 kWh battery

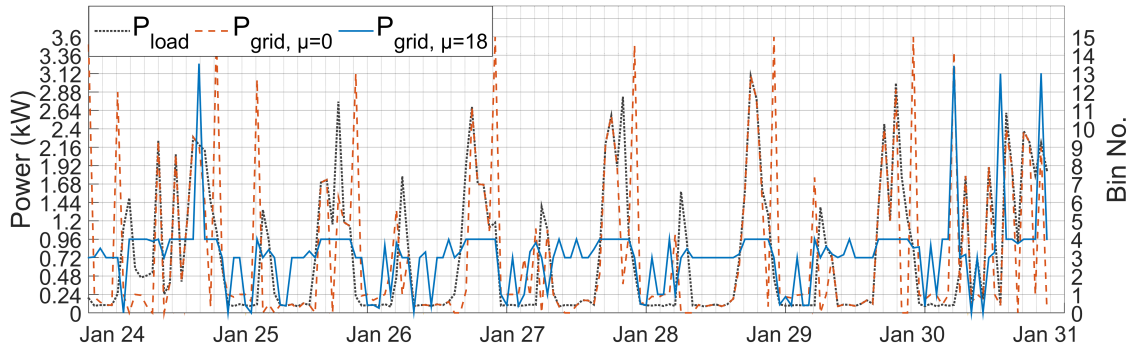
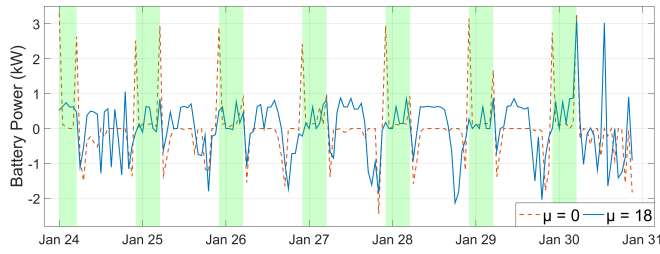
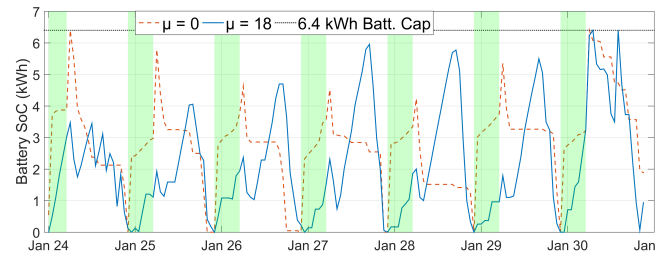


Fig. 3: Consumer vs grid load.

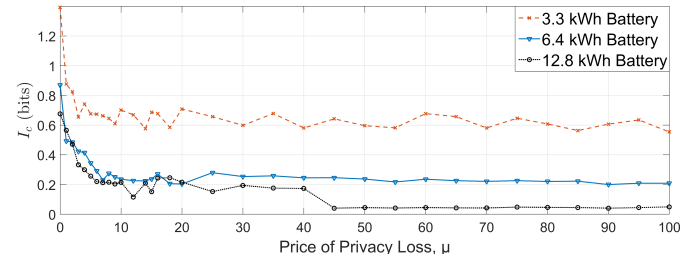


(a) Control actions of the battery

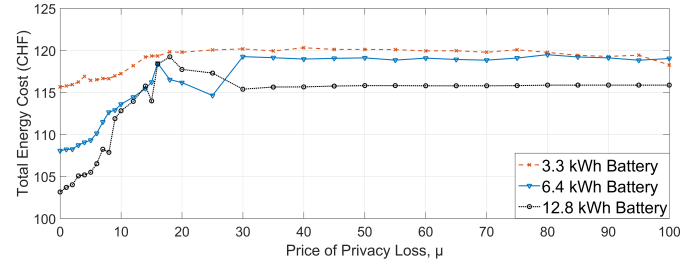


(b) Battery state of charge

Fig. 4: Control actions of the battery and its state of charge.



(a) Mutual information



(b) Total energy cost

Fig. 6: Comparison of different battery capacities.

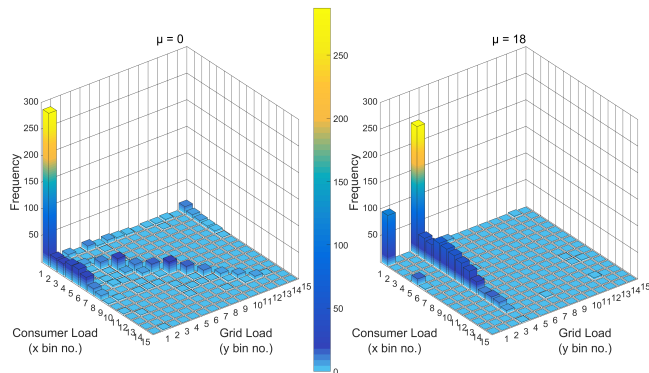


Fig. 5: Distribution of consumer and grid loads.

for energy cost optimization only is already approximately half that of the no-battery case.

Similar to the findings in [16], the size of the battery relative to the total consumer load over a high-low consumption cycle determines the level of privacy protection that can be achieved. Privacy loss is minimal with a battery capacity that sufficiently covers the consumer load during a typical day. In the case of the simulated consumer load, this battery capacity

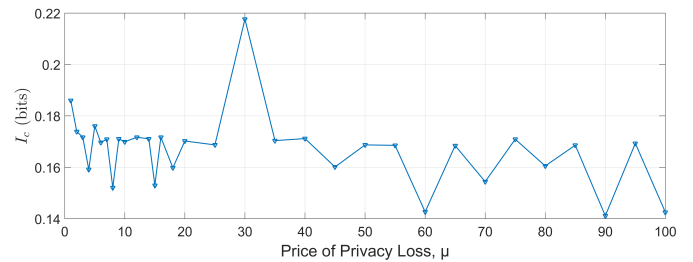


Fig. 7: Mutual information when energy cost is ignored.

is approximately 6.4 kWh, with a 12.8 kWh battery only achieving slightly better performance in terms of privacy loss reduction for moderate values of μ . However, energy cost reduction improves with a larger battery, since it also allows covering the consumption during periods of high energy price and low load.

As seen in Fig. 6(a), minimum privacy loss is achieved with a price of privacy loss of about 20 Rp/bit for a 6.4 kWh battery. Beyond this price of privacy loss, the system limitations (or the limitations of the measure I_c) impede the controller from doing better, and the mutual information is seen to fluctuate

around the minimum value. These fluctuations are caused by the inherent randomness that is present in the scheme, as well as due to the finiteness of the simulation period. This is seen Fig. 7, which shows how I_c varies as the price of privacy loss increases even when the energy cost is ignored. It can be seen that the “width” of these fluctuations is roughly 0.1 bits. They arise in part from the MIQP solver finding multiple solution candidates and choosing different ones, and hence affecting the system trajectory, purely due to the scaling of the objective function, which is completely controlled by μ when the energy cost is ignored.

The effect of the number of quantization levels of \tilde{X}_t and \tilde{Y}_t , which are m and n , respectively, and of the charge-discharge rate limit of the battery on the performance of the proposed controller were also studied. Fig. 8 shows I_c as a function of μ for different number of quantization levels and battery power ratings. For the evaluation of the quantization levels, $(m, n) = (20, 20)$ was used. Increasing the number of quantization levels for the same maximum load allows the controller to potentially achieve lower levels of privacy loss because it is now able to take advantage of the higher resolution to fine-tune its control actions. However, this also generally increases the fluctuation amplitude or variability of I_c due to the MIQP solver finding a larger set of candidate solutions. Nonetheless, smaller quantization levels could also result in large fluctuations when evaluated at higher resolutions due to the coarse level of controller actions, such as in the case of $(m, n) = (10, 10)$. The battery power ratings on the other hand impose a limit on the controller's ability to mask changes in consumer load. For the considered simulation setup with a maximum consumer load of 3.6 kW and a battery energy capacity of 6.4 kWh, a battery rating of 3.3 kW is almost sufficient. This can be seen in Fig. 8(b), where a battery with a 6.6 kW power rating marginally improves performance. A battery with a 1.65 kW rating is sufficient for lower prices of privacy loss, as energy cost reduction is the main driver of control actions in such cases. However, at higher prices of privacy loss the controller is unable to fully mask the consumer load peaks that occur mainly during high-energy-price periods, as shown in Fig. 4(a).

Additionally, as discussed in Section IV-A, a horizon length of $T = 12$ is insufficient for the controller to predict the load and fully charge the battery to minimize energy costs and mask consumer loads during the later stage of high energy price periods. Hence, the controller was simulated with different horizon lengths to study its performance and computational requirements. Table II and Fig. 9 summarize the results obtained. As can be seen from Fig. 9, prediction length mainly affects the energy cost because it allows the controller to anticipate consumer load that occur farther in the future. Increasing T to 18 reduces energy costs, and generally also reduces privacy-loss, due to the controller being able to fully utilize the capacity of the 6.4 kWh battery. However, there are exceptions to this due to the randomness in the scheme, which is exacerbated by longer horizons since they enlarge the solution space and increase the number of candidate MIQP solutions. It is important to note that computational tractability is still maintained with $T = 24$ despite having a median solver

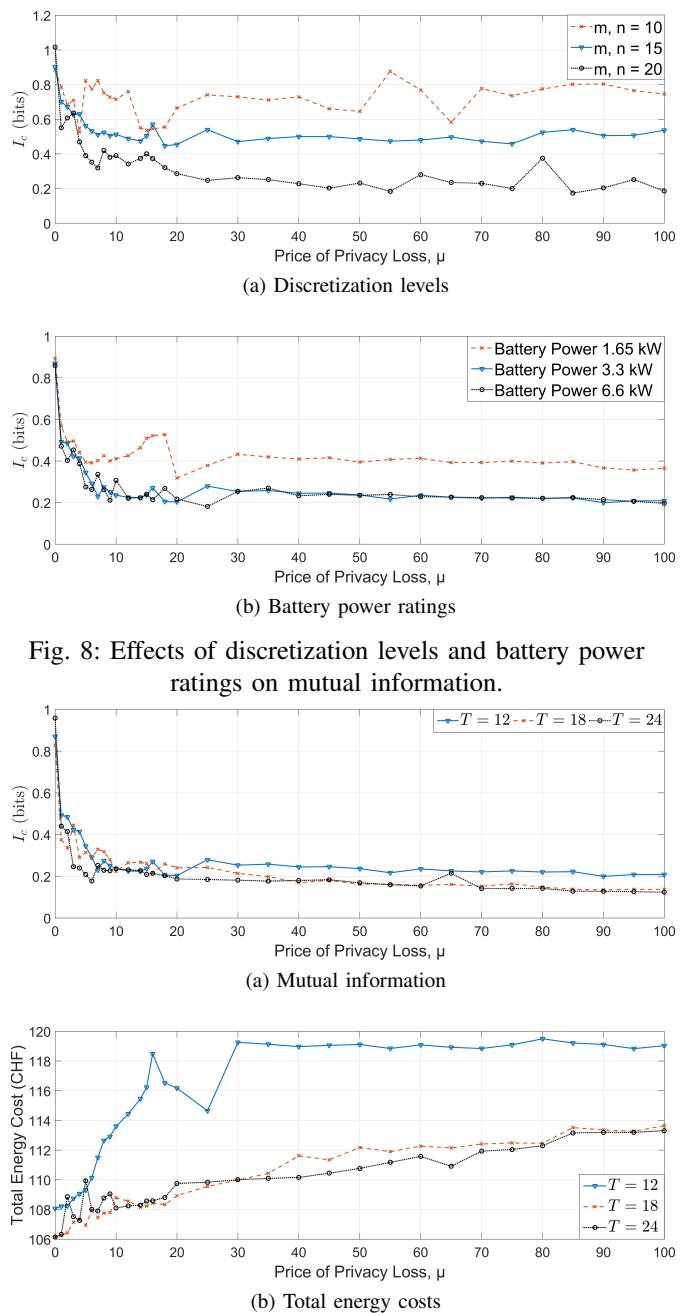


Fig. 8: Effects of discretization levels and battery power ratings on mutual information.

time of 57 times that of $T = 12$. However, as seen in Table II, the maximum solver time increases exponentially with the prediction horizon. Further increasing the horizon length to $T = 30$ makes it computationally impractical for a realistic controller as it requires more than one and a half hours using the current implementation to solve a single MIQP problem, which needs to be completed in under an hour to be practical. Note that for the energy pricing structure and consumer load profile in the simulation setting, a horizon length of 18 appears to be sufficient. However, this should not be generalized to other simulation settings and load profiles. In general, using the scheme proposed, a controller that is able to predict longer time periods while maintaining tractability should perform better.

TABLE II: Comparison Between Different Horizon Lengths.

	$\mu = 0$			$\mu = 15$			$\mu = 45$		
	$T = 12$	$T = 18$	$T = 24$	$T = 12$	$T = 18$	$T = 24$	$T = 12$	$T = 18$	$T = 24$
Max Solver Time (s)	0.072	0.085	0.112	1.14	11.0	152	1.39	11.4	211
Min Solver Time (s)	0.024	0.027	0.036	0.053	0.109	1.59	0.053	0.092	1.28
Mean Solver Time (s)	0.031	0.039	0.048	0.161	1.03	9.26	0.152	0.961	10.3
Median Solver Time (s)	0.030	0.036	0.045	0.126	0.712	5.64	0.117	0.667	5.60

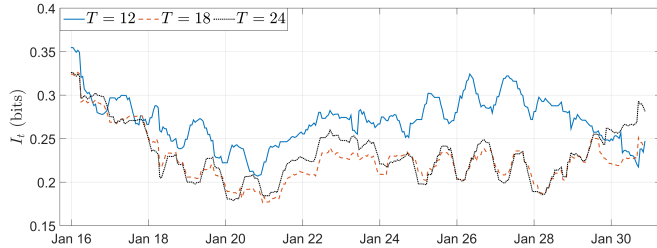


Fig. 10: Time series of mutual information with different prediction horizon lengths

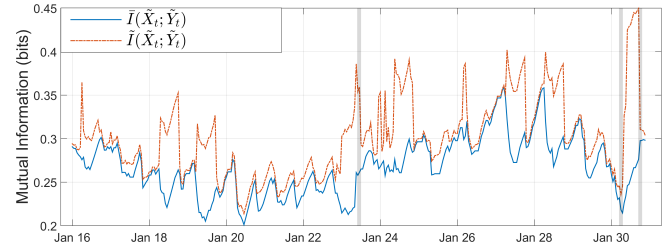


Fig. 11: Effects of logarithmic linearization

C. Time Evolution of Mutual Information

In order to study the change in mutual information with time, we evaluated the controller's performance with $\mu = 45$ for the three different horizon lengths discussed in Section IV-B using $\bar{I}(\tilde{X}_t; \tilde{Y}_t)$, *i.e.*, (11), with a moving window of length $N = 132$. This "time-dependent" approximation of mutual information is denoted by I_t . For each time t , the window considered the observation history from time $t - N + 1$ to time t , as shown in Fig. 2, hence it was based on the actual implemented controller actions. The graphs obtained of I_t are shown in Fig. 10. As seen from the plot, the results are consistent with the findings in Section IV-B, where longer horizon lengths also lead to generally lower mutual information over time. Note that mutual information does not change monotonically over time due to changing consumer load, the inherent randomness in the scheme, and the logarithm linearizations done by the controller, which make it overestimate the mutual information to varying degrees depending on the statistics of \tilde{X}_t and \tilde{Y}_t . The latter can be seen in Fig. 11, which now shows $\bar{I}(\tilde{X}_t; \tilde{Y}_t)$ with the time window $\{t - M + 1, \dots, t + T\}$ for $\mu = 20$ and $T = 12$, and the approximation with linearized logarithms used by the controller, (12), which is denoted by $\tilde{I}(\tilde{X}_t; \tilde{Y}_t)$. As seen on the plot, at certain times, the discrepancy introduced by the linearization leads to the controller taking actions that are expected to reduce mutual information, but in fact increase it. For example, this can be seen around the time corresponding to 11 AM on the 23rd of January and at 5 PM on the 30th of January. Around 6 AM on the 30th of January, on the other hand, this is reversed: mutual information is reduced when the controller predicted actions that supposedly increased mutual information. These periods are highlighted in grey on Fig. 11.

D. Comparison of MDPC and Load-Leveling

In the interest of comparing the performance of the proposed MDPC scheme against other BLH approaches, we imple-

mented a load-leveling scheme similar to the heuristic-driven approach in [15], but in an MPC setting with a dual objective to also minimise energy cost. More specifically, an MPC problem for this scheme consists of

$$\begin{aligned} & \underset{s, e, y, w}{\text{minimize}} && \frac{1}{T+1} \sum_{\tau=t}^{t+T} c_{\tau} y_{\tau} + \frac{\mu}{T+1} \sum_{\tau=t}^{t+T} (y_{\tau} - y_{\tau-1})^2 \\ & \text{subject to} && (s, e, y, w) \in \bar{\mathcal{F}}_t, \end{aligned}$$

where $(s, e, y, w) \in \bar{\mathcal{F}}_t$ enforces the system constraints (1), (2), (3) and (4), and the binary restrictions on w . Fig. 12 illustrates the trade-off between mutual information and energy cost for both the MDPC and Load-Leveling (LL) schemes for different battery capacities. As can be seen in Fig. 12, both schemes have increased energy costs with the reduction in mutual information, which is expected. When balancing between mutual information and energy cost, the MDPC scheme out-performs load-leveling, generally achieving lower mutual information for a similar cost of energy.

While both schemes are able to achieve similar levels of minimum privacy loss according to the proxy I_c for the different battery capacities, the resultant grid-load curves are quite different, as seen in Fig. 13. The grid load curve for the MDPC scheme shown in Fig. 13(a) no longer resembles the diurnal pattern of the actual consumer load, whereas this pattern can be clearly discerned from the load-leveling grid load curves shown in Fig. 13(b), which suggest that they should leak more information. These results strongly suggest that the mutual information proxy used by the MDPC scheme and for the evaluations is unable to capture these important properties, which is expected since they are related to time correlation. It is interesting (and perhaps surprising) that despite the proxy not being able to fully capture time correlation, the MDPC scheme is able mask the diurnal pattern in consumer load profiles.

V. CONCLUSION

In this paper, we proposed an MPC-based controller that balances energy costs and privacy protection based on mutual information. This is done by predicting the effects of the controller's actions on the statistics of the consumer load and that seen by the grid using counting, and solving MIQP problems of manageable size whenever new meter readings are available. While not computationally scalable with prediction horizon and discretization levels of load seen by the grid, the results obtained showed that the controller is able to reduce information leakage and hence protect consumer privacy. Extensive experiments were carried out in this work to thoroughly characterize the performance of the proposed controller. In particular, the effects of battery size, power ratings, prediction horizon lengths, and discretization were studied. Comparing the scheme against load-leveling also indicated an improvement in balancing between energy cost and consumer privacy protection. An important result of this work is that it shows that practical schemes that specifically target the minimization of a rigorous measure of privacy loss, such as the one proposed here, are possible.

Future work will focus on enlarging the reach of the prediction horizon, accounting for time correlation of the load consumptions, including more sophisticated probability estimation techniques, comparing the approach to other BLH schemes, and exploring MIQP relaxation methods to make the scheme more computationally scalable.

REFERENCES

- [1] European Union, "Directive of 2009/72/EC of the European Parliament and of the Council of 13 July 2009 Concerning Common Rules for the Internal Market in Electricity and Repealing Directive 2003/54/EC," *Official Journal of the European Union*, vol. L211, no. August, pp. 55 – 93, 2009.
- [2] E. L. Quinn, "Privacy and the New Energy Infrastructure," Tech. Rep. 09, 2009. [Online]. Available: <http://papers.ssrn.com/abstract=1370731>
- [3] P. McDaniel and S. McLaughlin, "Security and privacy challenges in the smart grid," *IEEE Security and Privacy*, vol. 7, no. 3, pp. 75–77, 2009.
- [4] G. W. Hart, "Residential energy monitoring and computerized surveillance via utility power flows," *IEEE Technology and Society Magazine*, vol. 8, no. 2, pp. 12–16, 1989.
- [5] H. Altrabalsi, J. Liao, L. Stankovic, and V. Stankovic, "A low-complexity energy disaggregation method: Performance and robustness," in *IEEE Symposium on Computational Intelligence Applications in Smart Grid (CIASG)*, 2014.
- [6] Z. Guanchen, G. Wang, H. Farhangi, and A. Palizban, "Residential electric load disaggregation for low-frequency utility applications," in *IEEE Power & Energy Society General Meeting*, 2015.
- [7] A. Molina-Markham, P. Shenoy, K. Fu, E. Cecchet, and D. Irwin, "Private memoirs of a smart meter," in *Proceedings of the 2nd ACM Workshop on Embedded Sensing Systems for Energy-Efficiency in Building*. Zurich, Switzerland: ACM, 2010, pp. 61–66.
- [8] M. A. Lisovich, D. K. Mulligan, and S. B. Wicker, "Inferring personal information from demand-response systems," *IEEE Security and Privacy*, vol. 8, no. 1, pp. 11–20, 2010.
- [9] U. Greveler, B. Justus, and D. Loehr, "Multimedia content identification through smart meter power usage profiles," *Computers, Privacy and Data Protection*, vol. 1, 2012.
- [10] S. McLaughlin, D. Podkuiko, S. Miazvezhanka, A. Delozier, and P. McDaniel, "Multi-vendor penetration testing in the advanced metering infrastructure," in *Proceedings of the 26th Annual Computer Security Applications Conference*, Austin, Texas, USA, 2010, pp. 107–116.
- [11] R. Hoenkamp, G. B. Huitema, and A. J. C. de Moor-van Vugt, "The neglected consumer: the case of the smart meter rollout in the Netherlands," *Renewable Energy Law and Policy Review*, no. 4, pp. 269–282, 2011.

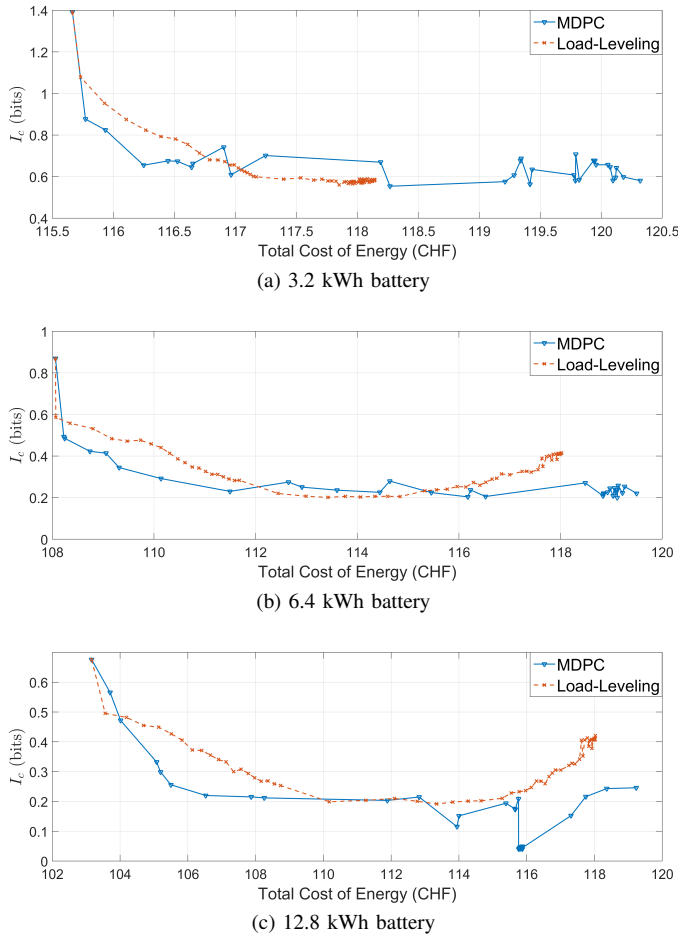


Fig. 12: Trade-off between I_c and energy cost of MDPC and Load-Leveling with different battery capacities

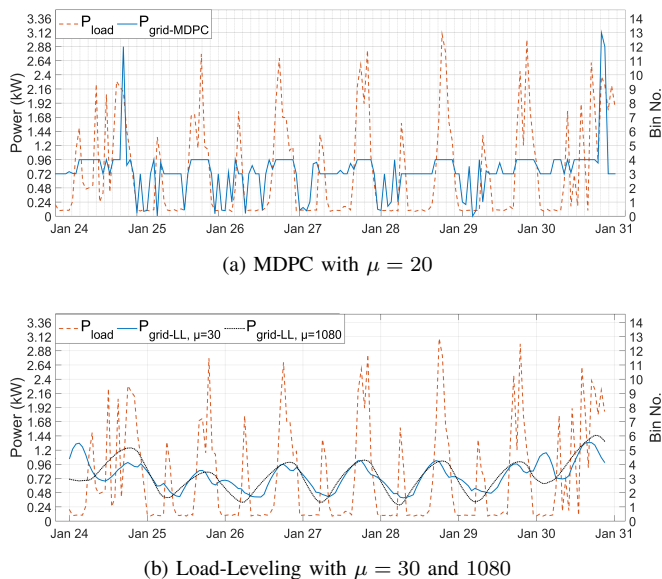


Fig. 13: Consumer vs grid load curves of MDPC and Load-Leveling

- [12] G. Acs and C. Castelluccia, "I have a DREAM! (Differentially PrivatE smart Metering)," *The 13th Information Hiding Conference (IH)*, pp. 118–132, 2011.
- [13] C. Dong, S. Kalra, D. Irwin, P. Shenoy, and J. Albrecht, "Preventing occupancy detection from smart meters," *IEEE Transactions on Smart Grid*, vol. 6, no. 5, pp. 2426–2434, 2015.
- [14] G. Kalogridis, C. Efthymiou, S. Z. Denic, T. A. Lewis, and R. Cepeda, "Privacy for Smart Meters: Towards Undetectable Appliance Load Signatures," in *First IEEE International Conference on Smart Grid Communications (SmartGridComm)*, 2010, pp. 232–237.
- [15] S. McLaughlin, P. McDaniel, and W. Aiello, "Protecting consumer privacy from electric load monitoring," in *Proceedings of the 18th ACM Conference Computer and Communications Security (CCS '11)*, Chicago, Illinois, USA, 2011, pp. 87–98.
- [16] W. Yang, N. Li, Y. Qi, W. Qardaji, S. McLaughlin, and P. McDaniel, "Minimizing private data disclosures in the smart grid," in *Proceedings of the 2012 ACM Conference on Computer and Communications Security (CCS '12)*. Raleigh, North Carolina, USA: ACM, 2012, p. 415.
- [17] G. Giaconi and D. Gunduz, "Smart meter privacy with renewable energy and a finite capacity battery," in *IEEE Workshop on Signal Processing Advances in Wireless Communications, SPAWC*, vol. 2016-August, Edinburgh, UK, 2016.
- [18] S. Li, A. Khisti, and A. Mahajan, "Structure of optimal privacy-preserving policies in smart-metered systems with a rechargeable battery," in *IEEE Workshop on Signal Processing Advances in Wireless Communications, SPAWC*, 2015, pp. 375–379.
- [19] O. Tan, D. Gunduz, and H. V. Poor, "Increasing smart meter privacy through energy harvesting and storage devices," *IEEE Journal on Selected Areas in Communications*, vol. 31, no. 7, pp. 1331–1341, 2013.
- [20] IRENA, "Battery Storage for Renewables: Market Status and Technology Outlook," Tech. Rep., 2015. [Online]. Available: http://www.irena.org/DocumentDownloads/Publications/IRENA_Battery_Storage_report_2015.pdf
- [21] A. Khakimova, A. Shamshimova, D. Sharipova, A. Kusatayeva, V. Ten, A. Bemporad, Y. Familiant, A. Shintemirov, and M. Rubagotti, "Hybrid model predictive control for optimal energy management of a smart house," in *IEEE 15th International Conference on Environment and Electrical Engineering (EEEIC)*, 2015, pp. 513–518.
- [22] W. Haiming, M. Ke, D. Zhao Yang, X. Zhao, L. Fengji, and W. Kit Po, "Efficient real-time residential energy management through MILP based rolling horizon optimization," in *IEEE Power & Energy Society General Meeting*, 2015.
- [23] A. Galka, T. Ozaki, and O. Yamashita, "A new approach to mutual information between pairs of times series," in *International Symposium on Nonlinear Theory and its Applications (NOLTA2005)*, Bruges, Belgium, 2005, pp. 626–629.
- [24] C. D. Manning, P. Raghavan, and H. Schütze, *An Introduction to Information Retrieval*. Cambridge University Press, 2009.
- [25] J. Löfberg, "Oops! I cannot do it again: Testing for recursive feasibility in MPC," *Automatica*, vol. 48, no. 3, pp. 550–555, 2012.
- [26] J. Lofberg, "YALMIP : a toolbox for modeling and optimization in MATLAB," in *IEEE International Conference on Computer Aided Control Systems Design*, 2004, pp. 284–289.
- [27] N. Pflugradt and W. Schufft, "Analysing low-voltage grids using a behaviour based load profile generator," *Renewable Energy and Power Quality Journal*, vol. 1, no. 11, pp. 1–5, 2013.



Systems Laboratory at ETH Zurich, with research emphasis on consumer privacy for smart metering systems, and short-term load forecasting.



His research consists on developing and applying mathematical optimization techniques for solving challenging problems, such as enabling large-scale integration of renewable energy in electric power grids. His employment experience includes Aurora Solar Inc. and the Electric Power Research Institute.



Her research is dedicated to the control and optimization of electric power systems.